LPV Analysis of a Gain Scheduled Control for an Aeroelastic Aircraft

Arnar Hjartarson, Peter Seiler and Gary J. Balas[1]

Abstract— **This paper considers the performance of a gain scheduled flight control law for an aeroelastic aircraft. A nonlinear aeroelastic model of the Rockwell B-1 Lancer is used as the application example. Gain scheduling via interpolation of point designs is the predominant method used in industry to develop a full-envelope flight control law. Certification and validation of these nonlinear gain-scheduled algorithms traditionally depends on linear metrics of robustness and massive nonlinear simulations efforts. The framework of Linear Parameter-Varying (LPV) systems offers a rigorous methodology for analysis that compliments traditional methods. New results on robust performance conditions in the LPV framework allows the analysis to take into account uncertainty in the aircraft model. The performance of the B-1 aircraft gain scheduled controller is evaluated using LPV metrics of robustness.**

I. INTRODUCTION

Lightweight flexible aircraft are a promising direction in aircraft design that has the potential to significantly increase aircraft fuel efficiency and operating range. Flexible aircraft require less structural mass than traditional aircraft, but the structural modes migrate to lower frequencies as the structure is made more flexible. Coupling between aerodynamic forces and the flexible modes of the aircraft structure (*aeroelasticity*) becomes a significant issue when the frequency of flexible modes falls inside the bandwidth of the aircraft's rigid body dynamics. In a worst-case scenario this coupling causes an uncontrollable oscillation, called *flutter*, in the aircraft structure that can destroy it.

The dynamic response of the flexible aircraft is hard to characterize because it depends on an accurate model of inertial, elastic and aerodynamic forces, and a correct representation of their coupling. These aeroelastic effects can be neglected in modeling of rigid aircraft but must be captured accurately for more flexible aircraft. The flight control law must be robust to aeroelastic effects as well as uncertainty in the approximate mathematical model.

Gain scheduling via interpolation of point designs is the predominant method used in industry to develop a full-envelope flight control law. Certification and validation of these nonlinear gain-scheduled algorithms traditionally depends on linear metrics of robustness, e.g. classical gain/phase/delay margins and/or MIMO robustness margins computed with the structured singular value, μ. It is important to note that classical robustness metrics assume linear time-invariant dynamics and hence time-variations between flight conditions are neglected. Evaluation of the system performance using Monte Carlo simulation techniques are often used to complement linear robustness analysis.

This paper considers a more rigorous robustness analysis for a gain-scheduled aeroelastic control system within the framework of Linear Parameter-Varying (LPV) systems. LPV systems are a class of linear systems where the state matrices depend on (measurable) time-varying parameters. The existing analysis results for such systems can roughly be categorized based on how the state matrices depend on the scheduling parameters. One approach is to assume the state matrices of the LPV system have a rational dependence on the parameters. In this case finite dimensional semidefinite programs (SDPs) can be formulated to assess the stability and input/output gain for the LPV system [1], [2], [3], [4]. An alternative approach is to assume the state matrices have an arbitrary dependence on the parameters. The analysis problem can be formulated as an infinite collection of parameter-dependent linear matrix inequalities (LMIs) [5], [6]. The latter approach is more suitable for the application to aeroelastic systems where the arbitrary dependence on the flight condition appears by linearization of nonlinear models.

An aeroelastic model of the Rockwell B-1 Lancer is used as the application example for the robustness analysis [7], [8]. This aircraft had ride quality issues due to aeroelastic phenomena and a special structural mode control system was designed to deal with its aeroelastic issues. The performance, robustness and worst-case performance of this gain-scheduled controller will be analyzed in this paper across the flight envelope using the LPV framework. As noted above, uncertainty in the model plays a significant role for aeroelastic vehicles. The robust performance condition in [9] for uncertain LPV systems will be applied. This analysis result applies to LPV systems with arbitrary dependence on the parameters and uses the Integral Quadratic Constraint (IQC) [10] framework to model the uncertainty. Similar IQCs robustness results for LPV systems whose state matrices have rational dependence on the scheduling parameters can be found in [11], [12].

The LPV framework is well suited for aeroelastic systems because it can handle the variation in the aircraft dynamics with flight condition. This allows the analysis to take into account drastic changes in flutter modes across the flight envelope. The robust performance conditions add the capability of accounting for uncertainty in the dynamics when working in the LPV framework. Hence, uncertainty in the models of flexible modes, and their coupling with the aerodynamics, can be included explicitly in the analysis. The robust performance condition in [9] is chosen for this

[1]Arnar Hjartarson is with MUSYN Inc., Minneapolis, MN 55414, USA arnar.hjartarson@musyn.com

Peter Seiler is with MUSYN Inc., Minneapolis, MN 55414, USA peter.j.seiler@gmail.com

Gary J. Balas is with MUSYN Inc., Minneapolis, MN 55414, USA balas@musyn.com

analysis because in it the parameter dependence of the LPV model does not need to be modeled explicitly. The nonlinear simulation model is linearized on a grid of parameter values that spans the flight envelope, to yield look-up tables that describe the dynamics of the nonlinear model at each point on the grid. This formulation allows for arbitrary dependence of the dynamics on the scheduling parameters. This approach to robust performance analysis in the LPV framework is a natural extension of analysis involving traditional linear metrics of performance which rely on the same look-up tables of linearized dynamics.

II. TECHNICAL BACKGROUND

A. LPV Systems

Linear parameter varying (LPV) systems are a class of systems whose state space matrices depend on a time-varying parameter vector $\rho : \mathbb{R}^+ \to \mathbb{R}^{n_\rho}$. The parameter is assumed to be a continuously differentiable function of time and admissible trajectories are restricted, based on physical considerations, to a known compact subset $\mathscr{P} \subset \mathbb{R}^{n_\rho}$. In addition, the parameter rates of variation $\dot{\rho} : \mathbb{R}^+ \to \dot{\mathscr{P}}$ are assumed to lie within a hyperrectangle $\dot{\mathscr{P}}$ defined by

$$\dot{\mathscr{P}} := \{q \in \mathbb{R}^{n_\rho} \mid \underline{\nu}_i \le q_i \le \bar{\nu}_i,\ i = 1,\ldots,n_\rho\}. \tag{1}$$

The set of admissible trajectories is defined as $\mathscr{A} := \{\rho : \mathbb{R}^+ \to \mathbb{R}^{n_\rho} \ : \ \rho(t) \in \mathscr{P},\ \dot{\rho}(t) \in \dot{\mathscr{P}}\ \forall t \ge 0\}$. The parameter trajectory is said to be rate unbounded if $\dot{\mathscr{P}} = \mathbb{R}^{n_\rho}$.

The state-space matrices of an LPV system are continuous functions of the parameter: $A : \mathscr{P} \to \mathbb{R}^{n_x \times n_x}$, $B : \mathscr{P} \to \mathbb{R}^{n_x \times n_d}$, $C : \mathscr{P} \to \mathbb{R}^{n_e \times n_x}$ and $D : \mathscr{P} \to \mathbb{R}^{n_e \times n_d}$. An n_x^{th} order LPV system, G_ρ, is defined by

$$\begin{aligned} \dot{x}(t) &= A(\rho(t))x(t) + B(\rho(t))d(t) \\ e(t) &= C(\rho(t))x(t) + D(\rho(t))d(t) \end{aligned} \tag{2}$$

Hence, LPV systems represent a special class of time-varying systems. The explicit dependence on t is occasionally suppressed to shorten the notation.

B. Integral Quadratic Constraints

IQCs were introduced in [10] to provide a general framework for robustness analysis. An IQC is defined by a symmetric matrix $M = M^T \in \mathbb{R}^{n_z \times n_z}$ and a stable linear system $\Psi \in \mathbb{RH}_\infty^{n_z \times (m_1+m_2)}$. Ψ is denoted as

$$\Psi(j\omega) := C_\psi(j\omega I - A_\psi)^{-1}[B_{\psi 1}\ B_{\psi 2}] + [D_{\psi 1}\ D_{\psi 2}] \tag{3}$$

A bounded, causal operator $\Delta : \mathscr{L}_{2e}^{m_1} \to \mathscr{L}_{2e}^{m_2}$ satisfies an IQC defined by (Ψ, M) if the following inequality holds for all $v \in \mathscr{L}_2^{m_1}[0,\infty)$, $w = \Delta(v)$ and $T \ge 0$:

$$\int_0^T z(t)^T M z(t)\, dt \ge 0 \tag{4}$$

where z is the output of the linear system Ψ:

$$\dot{x}_\psi(t) = A_\psi x_\psi(t) + B_{\psi 1} v(t) + B_{\psi 2} w(t),\ x_\psi(0) = 0 \tag{5}$$

$$z(t) = C_\psi x_\psi(t) + D_{\psi 1} v(t) + D_{\psi 2} w(t) \tag{6}$$

The notation $\Delta \in IQC(\Psi, M)$ is used if Δ satisfies the IQC defined by (Ψ, M).

Reference [10] provides a library of IQC multipliers that are satisfied by many important system components, e.g. saturation, time delay, and norm bounded uncertainty. The IQCs in [10] are expressed in the frequency domain as an integral constraint defined using a multiplier Π. The multiplier Π can be factorized as $\Pi = \Psi^* M \Psi$ and this connects the frequency domain formulation to the time-domain formulation used in this paper. One technical point is that, in general, the time domain IQC constraint only holds over infinite horizons ($T = \infty$). The work in [10], [13] draws a distinction between hard/complete IQCs for which the integral constraint is valid over all finite time intervals and soft/conditional IQCs for which the integral constraint need not hold over finite time intervals. The formulation of an IQC in this paper as a finite-horizon (time-domain) inequality is thus valid for any frequency-domain IQC that admits a hard/complete factorization (Ψ, M). While this is somewhat restrictive, it has recently been shown that a wide class of IQCs have a hard factorization [13]. The remainder of the paper will simply treat, without further comment, (Ψ, M) as the starting point for the definition of the finite-horizon IQC.

C. LPV Robustness Analysis

This section briefly summarizes the main technical result in [9] which provides a parameterized linear matrix inequality (LMI) condition to assess the robustness of an uncertain LPV systtem. An uncertain LPV system is described by the interconnection of an LPV system G_ρ and an uncertainty Δ, as depicted in Figure 1. This interconnection represents an upper linear fractional transformation (LFT), which is denoted $\mathscr{F}_u(G_\rho, \Delta)$. The uncertainty Δ is assumed to satisfy an IQC described by (Ψ, M). Note that the perturbation Δ can include hard nonlinearities (e.g. saturations) and infinite dimensional operators (e.g. time delays) in addition to true system uncertainties. The term "uncertainty" is used for simplicity when referring to the the perturbation Δ.

The robust performance of $\mathscr{F}_u(G_\rho, \Delta)$ is measured in terms of the worst case induced $\mathscr{L}_2$ gain from the input d to the output e. The worst-case gain is defined as

$$\sup_{\substack{\Delta \in IQC(\Psi, M) \\ \rho(\cdot) \in \mathscr{A}}} \|\mathscr{F}_u(G_\rho, \Delta)\|. \tag{7}$$

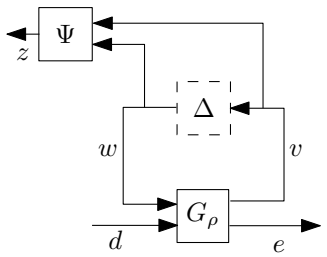

Fig. 1. Analysis Interconnection Structure

The analysis interconnection in Figure 1 includes the filter Ψ. The dynamics of this interconnection are described by

$w = \Delta(v)$ and

$$\begin{aligned} \dot{x} &= A(\rho)x + B_1(\rho)w + B_2(\rho)d \\ z &= C_1(\rho)x + D_{11}(\rho)w + D_{12}(\rho)d \\ e &= C_2(\rho)x + D_{21}(\rho)w + D_{22}(\rho)d, \end{aligned} \tag{8}$$

where the state vector is $x = [x_G; x_\psi]$ with x_G and x_ψ being the state vectors of the LPV system G_ρ and the filter Ψ respectively. The uncertainty Δ is shown in the dashed box in Figure 1 to signify that it is removed for the analysis. The signal w is treated as an external signal subject to the constraint in Equation 4. This effectively replaces the precise relation $w = \Delta(v)$ with the quadratic constraint on z.

A dissipation inequality can be formulated to upper bound the worst-case $\mathscr{L}_2$ gain of $\mathscr{F}_u(G_\rho, \Delta)$ using the system Equation 8 and the time domain IQC Equation 4.

Theorem 1: [9] Assume $\mathscr{F}_u(G_\rho, \Delta)$ is well posed for all $\Delta \in \mathrm{IQC}(\Psi, M)$. Then the worst-case gain is $\leq \gamma$ if there exists a continuously differentiable $P : \mathscr{P} \to \mathbb{S}^{n_x}$ and a scalar $\lambda > 0$ such that $\forall (p,q) \in \mathscr{P} \times \dot{\mathscr{P}}$, $P(p) > 0$,

$$\begin{aligned} &\begin{bmatrix} P(p)A(p) + A(p)^T P(p) + \partial P(p,q) & P(p)B_1(p) & P(p)B_2(p) \\ B_1(p)^T P(p) & 0 & 0 \\ B_2(p)^T P(p) & 0 & -I \end{bmatrix} + \\ &\quad + \lambda \begin{bmatrix} C_1(p)^T \\ D_{11}(p)^T \\ D_{12}(p)^T \end{bmatrix} M \begin{bmatrix} C_1(p) & D_{11}(p) & D_{12}(p) \end{bmatrix} \\ &\quad + \frac{1}{\gamma^2} \begin{bmatrix} C_2(p)^T \\ D_{21}(p)^T \\ D_{22}(p)^T \end{bmatrix} \begin{bmatrix} C_2(p) & D_{21}(p) & D_{22}(p) \end{bmatrix} < 0 \end{aligned} \tag{9}$$

where ∂P is defined as: $\partial P(p,q) = \sum_{i=1}^{n_\rho} \frac{\partial P(p)}{\partial p_i} q_i$

III. B-1 AIRCRAFT

The Rockwell B-1 Lancer is a supersonic bomber that was introduced in the 1970s. The B-1 has four turbofan engines and variable wing sweep. The aircraft is equipped with control surfaces on the vertical and horizontal stabilizer, as well as spoilers on the wings. The B-1 had serious ride quality issues at subsonic speeds due to aeroelastic effects. These issues were resolved by adding canard control surfaces to the front of the aircraft, controlled by a dedicated Structural Mode Control System (SMCS) that uses them to damp out the aircraft's flexible modes. The aeroelastic issues seen on the B-1 spurred an interest in modeling and control of aeroelastic aircraft. Several papers that aimed at modeling the B-1 aircraft's aeroelastic issues were published in the 1970s and 1980s [14], [15], [16], [17], [18].

A. Nonlinear Simulation Model

A nonlinear simulation model approximating the B-1 aircraft was developed in Simulink from data in the open literature and made freely available online [8]. The objective for the development of this nonlinear simulation is to provide the community with a benchmark example of an aeroelastic aircraft. The nonlinear simulation model includes six rigid body degrees of freedom, and five elastic degrees of freedom. Each of the flexible modes has two states associated with it: $x_e = (e_1, \dot{e}_1, e_2, \dot{e}_2, e_3, \dot{e}_3, e_4, \dot{e}_4, e_5, \dot{e}_5)$ Where e_i denotes the generalized coordinate associated with the ith elastic mode. Modes e_1, e_2 and e_3 describe the three lowest-frequency symmetric elastic modes of the B-1 aircraft, while modes e_4 and e_5 describe the two lowest-frequency anti-symmetric elastic modes. The first symmetric (e_1) and the second anti-symmetric mode (e_5) contribute most to the vibrations that are felt in the cockpit, which necessitated the addition of the canards and SMCS.

The states associated with the rigid body dynamics are U, V, W, p, q, r, ϕ, θ and ψ, which represent the x-, y-, and z-axis velocity expressed in the body-coordinate system, the roll, pitch, and yaw rate at the aircraft Center of Gravity (CG), and the bank angle, pitch angle and yaw angle of the aircraft, respectively. The simulation includes measurements of the states associated with the rigid body dynamics, as well as a measurement of the aircraft's airspeed V_T, angle of attack α, sideslip angle β, lateral acceleration at the CG and cockpit, $n_{y,cg}$ and $n_{y,cp}$ respectively, and vertical acceleration at the CG and cockpit, $n_{z,cg}$ and $n_{z,cp}$ respectively.

B. Control Systems

The B-1 aircraft is equipped with a Stability Augmentation System (SAS) [19], [20], [16], and a Structural Mode Control System (SMCS) [19], [20]. This paper will focus on the longitudinal dynamics of the B-1 aircraft, and the pitch axis SAS and plunge axis SMCS.

The pitch axis SAS is used to shape the stick-to-pitch rate response of the aircraft and tune the aircraft's short-period mode to deliver satisfactory natural frequency and damping across the flight envelope. It takes in stick input for pitch, q_{ref} [deg], a measurement of the pitch rate, q [deg/s], and outputs a deflection command to the horizontal stabilizer, δ_H [deg],

$$\delta_H = K_q(h)q + q_{ref} \tag{10}$$

The SAS is a gain scheduled controller, and the K_q gain is scheduled on altitude, h [ft],

$$K_q(h) = 0.306 + \frac{0.544}{55000}h \tag{11}$$

The SMCS was added to the B-1 to damp out the elastic modes of the aircraft, and prevent an unacceptable level of cockpit vibration. The plunge axis SMCS (Figure 2) takes in vertical accelerations at the aircraft's center-of-gravity and cockpit, $n_{z,cg}$ [ft/s^2] and $n_{z,cp}$ [ft/s^2] respectively, and outputs deflection commands to the canard control vanes, δ_{cvsym} [deg]. The plunge axis SMCS is a gain scheduled

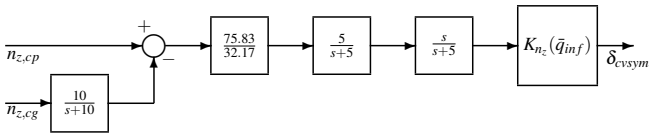

Fig. 2. Interconnection of the gain-scheduled plunge axis SMCS.

controller, and the $K_{n_z}(\bar{q}_{inf})$ gain is scheduled on dynamic pressure, $\bar{q}_{inf}$ [psf], as seen in Figure 3.

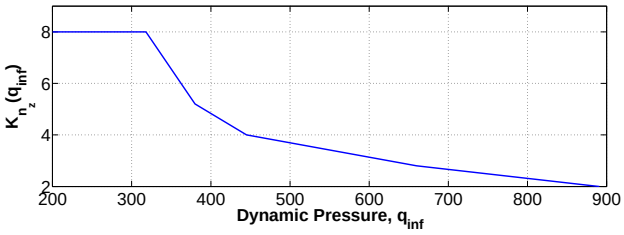

Fig. 3. The $K_{n_z}(\bar{q}_{inf})$ gain in the plunge axis SMCS.

IV. PROBLEM FORMULATION

A. Linearization

This paper investigates the performance of the B-1 gain-scheduled control system as the aircraft flies at Mach numbers between 0.6 and 0.8, and altitudes between 5,000 ft and 10,000 ft. The nonlinear simulation model of the B-1 aircraft is trimmed and linearized at a straight and level flight condition on the grid $(\text{Mach}, \text{altitude}) = [0.6, 0.7, 0.8] \times [5000,\ 10000]$ ft. These flight conditions describe the flight envelope for this analysis. The SIMULINK model is trimmed using the `findop` function in MATLAB, and linearized using the `linearize` function. The linearization procedure yields a 3×2 grid of linearized models arranged by Mach and altitude values.

This paper will focus on the longitudinal dynamics of the B-1 aircraft, and utilize a reduced order model of the B-1. The lateral and longitudinal dynamics of the B-1 aircraft exhibit minimal coupling at the flight conditions where the model was linearized. Hence, a longitudinal model of the B-1 aircraft is extracted at each linearization point by removing the states associated with the lateral dynamics: V, p, r, ϕ, e_4, $\dot{e}_4$, e_5, and $\dot{e}_5$. These states are truncated from the model.

The longitudinal dynamics of the B-1 aircraft are dominated by the short period and phugoid modes, and by the lowest frequency elastic mode (e_1). The analysis in this paper will focus on the frequency range which encompasses these modes. Hence, the h, e_2, $\dot{e}_2$, e_3, and $\dot{e}_3$ states are removed from the model because their dynamics have minimal effects in this frequency range. These states are truncated from the model, to yield a reduced order model of the B-1 aircraft's longitudinal dynamics, represented by the U, W, q, θ, e_1, and $\dot{e}_1$ states.

These linearized models are used to form an LPV model of the B-1 aircraft that is scheduled on altitude and Mach. Together the linear models form a grid-based LPV model of the aircraft dynamics, in the form of equation 2, that can be used for analysis in the LPV framework [5], [9], [21]. The gain-scheduled SAS and SMCS control laws are likewise evaluated at each of these grid points, and modeled in LPV form to correspond to the LPV B-1 aircraft model.

B. Model Matching Performance Problem

The performance of the gain-scheduled controller across the prescribed flight envelope is of interest. The controller performance is evaluated in the LTI framework at individual linearization points using traditional metrics of performance (e.g. Gain and Phase Margins, μ). The performance of the gain-scheduled controller is also evaluated analytically through a model-matching formulation, using the LPV framework described in Section II.

In this model matching formulation, the desired response of the closed-loop system is characterized by a reference model, which the output of the actual closed-loop system is compared against. The performance of the gain-scheduled controller is measured by the error between the reference model and the output of the closed-loop system. This error is measured by the induced $\mathscr{L}_2$ norm of the model matching interconnection.

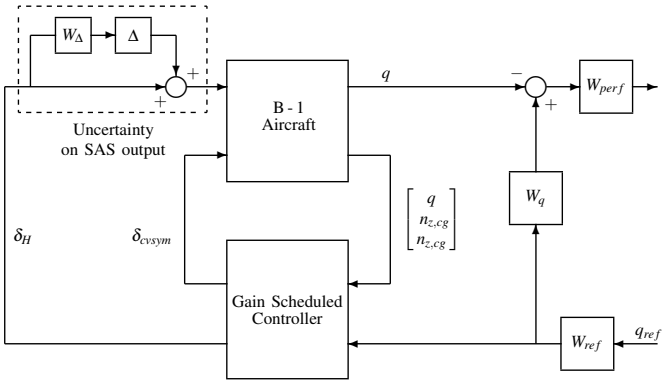

Fig. 4. Interconnection for B-1 aircraft model matching formulation.

Figure 4 shows the interconnection that forms the model-matching problem that is studied here. The focus is on the stick-to-pitch rate response achieved by the combined SAS and SMCS. This response is dominated by the short-period mode, the phugoid mode, and aeroelastic effects associated with the lowest frequency elastic mode (e_1). Hence, the weights used in the model matching problem are selected to focus the analysis on the 0.05 rad/s - 11 rad/s frequency range, where the performance of the SAS and SCMCS is most critical.

W_{ref} weights the input stick command. W_{ref} is chosen to be a first order system: $W_{ref} = \frac{10}{s+10}$, which limits the stick command input to 10 rad/s, where W_{ref} starts to roll off.

W_q is the reference model that defines the desired stick-to-pitch rate response of the vehicle. The reference model is chosen to match the pitch rate response of the closed-loop system at Mach = 0.7 and h = 5000 ft in the frequency range 0.05 rad/s - 11 rad/s. W_q is a combination of three second order systems: The first describes the short period mode and has a zero at -0.563, and poles at $-1.92 \pm 0.977j$. The second approximates the phugoid mode and has zeros at $-0.016 \pm 0.022j$, and poles at $-0.007 \pm 0.086j$. The third approximates the effects of the lowest frequency elastic mode (e_1) and has zeros at $-0.73 \pm 7.845j$, and poles at $-2.135 \pm 10.77j$. The gain of the combined system is -11.4.

The permissible error in the pitch rate response is characterized by the weight W_{perf}, which acts on the difference between the reference model and the output of the closed-loop system. The pitch rate response of the closed-loop system due to a q_{ref} command should closely match that

of W_q in the frequency range of interest. Hence, the W_{perf} weight is chosen such that the error between the reference system and the closed-loop response is less than 10% at 0.05 - 11 rad/s,

$$W_{perf} = \frac{110s}{(s+0.05)(s+11)} \tag{12}$$

A multiplicative input uncertainty is added to the output of the SAS in the model matching performance problem. This multiplicative dynamic uncertainty $||\Delta(s)||_\infty \leq 1$, is weighted by $W_\Delta \in \mathbb{R}^+$. W_Δ is a bound on the magnitude of the uncertainty in the δ_H channel: $||\Delta(s)W_\Delta||_\infty \leq W_\Delta$.

The model matching interconnection will be used to evaluate the performance of the B-1 gain-scheduled flight controller in both the LTI and LPV framework.

V. ANALYSIS RESULTS

A. Software

MUSYN Inc. is developing a software tool, LPVTools, to aid in modeling, analysis, controller synthesis, and simulation of LPV systems. LPVTOOLS is a software suite that provides parameter-varying data structures for modeling of LPV systems within the MATLAB/SIMULINK software environment, and extends the functionality of standard functions from Control System and Robust Control Toolbox to the LPV framework [22]. Tools specific to the LPV framework are also provided, to aid in model reduction, analysis and control design. The LPVTOOLS software is used to generate all the results in the LPV framework in this paper.

B. Core Analysis

The closed-loop LTI system formed by the linearized B-1 aircraft model and the linearized SAS, and SMCS controllers can be analyzed at each trim point: (Mach, Altitude) $\in [0.6, 0.7, 0.8] \times [5{,}000\,\text{ft}, 10{,}000\,\text{ft}]$. Each closed-loop system describes the dynamics of the aircraft as it cruises straight and level at a fixed speed and altitude.

The gain and phase margins of the closed-loop system are computed channel-by-channel for both the inputs and outputs of the B-1 model. The gain and phase margins at the input to the B-1 model are obtained by breaking the closed-loop where the δ_H and δ_{cvsym} commands enter the model, and margins at the output are obtained by breaking the closed-loop where the q, $n_{z,cg}$ and $n_{z,cp}$ measurements exit the model. The gain-scheduled controllers yield adequate gain and phase margins. The gain margins are larger than 6 dB and the phase margins are larger than 28 deg, for each input/output channel at every flight condition.

The effect of the modeled uncertainty is studied by computing the worst-case gain of the model matching interconnection shown in Figure 4. An LTI model matching interconnection is formed at each Mach and altitude grid point for analysis. The worst-case gain is computed using the command `wcgain` in the Robust Control Toolbox in MATLAB. Figure 5 shows how the worst-case gain changes as a function of the uncertainty magnitude W_Δ at (Mach, Altitude) $\in [0.6, 0.8] \times [5{,}000\,\text{ft}, 10{,}000\,\text{ft}]$. In terms of robust performance, the closed-loop system is least robust at Mach = 0.6 and altitude = 5,000 ft, where it can tolerate 20% dynamic uncertainty before the error grows beyond the prescribed limit.

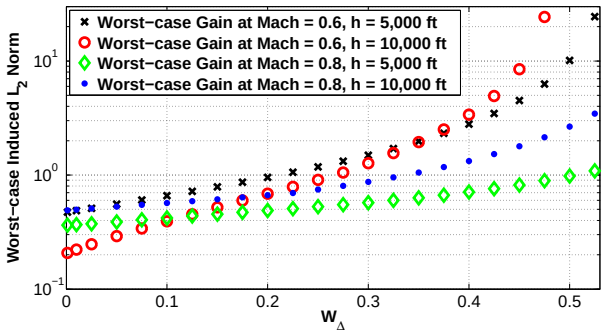

Fig. 5. Induced $\mathscr{L}_2$ norm of LTI model matching interconnection as a function of uncertainty, at fixed Mach and altitude.

The LPV framework allows the analysis to take into account the time-varying nature of both the aircraft dynamics and the gain-scheduled controller, as they change with altitude and Mach. In this case the LPV models of the B-1 aircraft, and the SAS and SMCS controllers are used to form the model matching interconnection in LPV form. The LPV model matching interconnection is used to evaluate the performance of the nonlinear gain-scheduled controller across the whole grid of altitude and Mach values simultaneously. Both the nominal LPV interconnection (no uncertainty), and the uncertain LPV interconnection (with uncertainty) are used in the analysis.

Figure 6 shows the upper bound on the induced $\mathscr{L}_2$ norm of the nominal LPV model matching interconnection (no uncertainty). The induced $\mathscr{L}_2$ norm grows with permissible rate of change in Mach, but the change in the norm due to the rate of change in altitude is very small within the modeled flight envelope. The gain-scheduled controller maintains the desired performance for climb/descent rates of 800 ft/s and $\frac{d}{dt}\text{Mach} \leq 0.06$ (equivalent to approximately 66 ft/s^2 rate of change in airspeed at the modeled flight conditions).

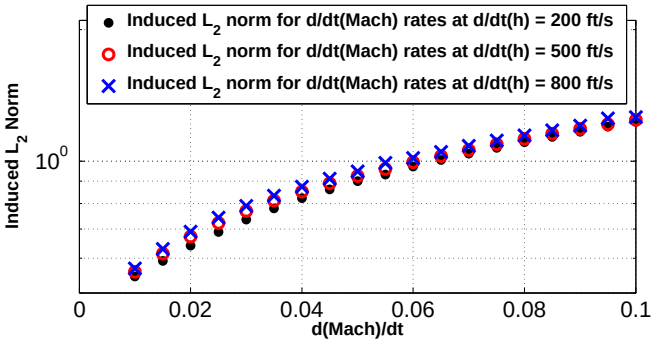

Fig. 6. Induced $\mathscr{L}_2$ norm of LPV model matching interconnection.

Figure 7 shows the upper bound on the worst-case induced $\mathscr{L}_2$ norm of the uncertain LPV model matching interconnection. As seen in Figure 7, the performance specification, of having the error in the pitch rate response of the closed-loop

system remain less than 10% in the target frequency range, can not be met for $\frac{d}{dt}\text{Mach} = 0.1$ and $\dot{h} = 200$ ft/s. In contrast, the controller will achieve robust performance for up to 15% dynamic uncertainty for $\frac{d}{dt}\text{Mach} \leq 0.01$ and $\dot{h} = 200$ ft/s.

The LTI worst-case gain results shown in Figure 5, predicted robust performance to at least 20% dynamic uncertainty in the SAS output. However, the LPV worst-case gain results in Figure 7 indicate that the gain-scheduled controller becomes less robust to uncertainty as the rate of change in Mach grows.

The algorithm to find the worst-case induced $\mathscr{L}_2$ norm of an LPV system is only capable of finding an upper bound on the norm, and not a lower bound. Without a rigorous way of finding the lower bound for a worst-case norm of a LPV system, the lower bound can be approximated by bounding the norm from below by the norm of the nominal LPV system. The solid blue line in Figure 7 shows the induced $\mathscr{L}_2$ norm of the nominal LPV system at $\frac{d}{dt}\text{Mach} \leq 0.01$ and $\dot{h} = 200$ ft/s. When the uncertainty is very small the worst-case norm of the uncertain LPV system converges to the norm of the nominal LPV system.

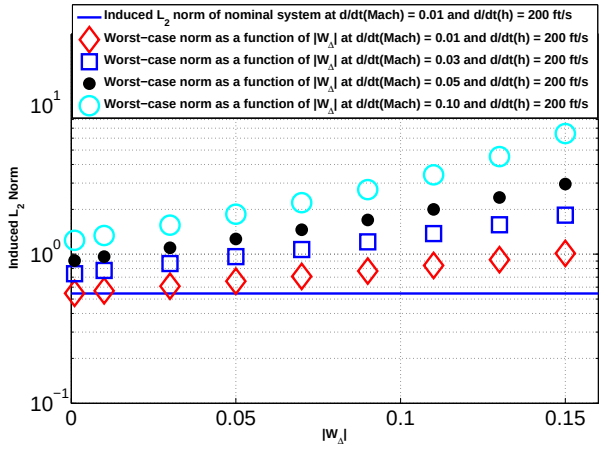

Fig. 7. Induced $\mathscr{L}_2$ norm of uncertain LPV model matching interconnection

In summary, Figure 5 shows that as the aircraft cruises at straight and level, and at fixed speed and altitude, the gain-scheduled controller will achieve the desired level of performance at each (Mach,altitude) grid point, in the presence of up to 20% uncertainty in the SAS output. Figure 6 shows that the gain-scheduled controller can maintain this performance at very aggressive $\frac{d}{dt}\text{Mach}$ and $\dot{h}$ rates when there is no uncertainty in the system. Figure 7 illustrates that performance degrades when the aircraft is subjected to simultaneous variations in altitude and Mach, with uncertainty. For relatively small rates of change in Mach and altitude the level of uncertainty that can be tolerated while meeting the desired level of performance is lowered significantly (e.g. for $\frac{d}{dt}\text{Mach} \leq 0.01$ and $\dot{h} = 200$ ft/s, the tolerable level of uncertainty is only 15%, instead of 20% as in LTI case.)

VI. CONCLUSIONS

This paper analyzed a gain-scheduled controller for an aeroelastic aircraft. The analysis shows that the controller performs well across the modeled flight domain. Its performance is guaranteed analytically for various climb/descent rates and rates of change of Mach, using the LPV framework. Further work will extended the analysis to include the lateral-directional dynamics, and study the effects of uncertainty in the aircraft aerodynamic coefficients and elastic modes. Further work is also needed to derive conditions for the lower bounds on the worst-case induced $\mathscr{L}_2$ norm for LPV systems.

ACKNOWLEDGMENT

This work was supported by a NASA Small Business Innovative Research contract from NASA Armstrong Flight Research Center, contract #NNX12CA14C. Contract Monitor is Dr. Martin J. Brenner. The authors thank Dr. David K. Schmidt for sharing his insights about the B-1 aircraft and for developing the nonlinear simulation used in this work.

REFERENCES

[1] A. Packard, "Gain scheduling via linear fractional transformations," *Systems and Control Letters*, vol. 22, no. 2, pp. 79–92, 1994.
[2] P. Apkarian and P. Gahinet, "A convex characterization of gain-scheduled H_∞ controllers," *IEEE TAC*, vol. 40, no. 5, 1995.
[3] ——, "Erratum to "A convex characterization of gain-scheduled H_∞ controllers"," *IEEE TAC*, vol. 40, no. 9, 1995.
[4] C. W. Scherer, "Advances in linear matrix inequality methods in control." SIAM, 2000, ch. Robust mixed control and linear parameter-varying control with full block scalings, pp. 187–207.
[5] F. Wu, "Control of linear parameter varying systems," Ph.D. dissertation, University of California, Berkeley, 1995.
[6] F. Wu, X. H. Yang, A. Packard, and G. Becker, "Induced $\mathscr{L}_2$ norm control for LPV systems with bounded parameter variation rates," *Int. J. Robust. Nonlinear Control*, vol. 6, pp. 983–998, 1996.
[7] D. K. Schmidt, *Modern flight dynamics*. McGraw-Hill, 2012.
[8] ——, "FLEXSIM Nonlinear Simulation," 2013, Available: http://highered.mcgraw-hill.com/sites/007339811x/student_view0/matlab_files.html and http://www.musyn.com.
[9] H. Pfifer and P. Seiler, "Robustness analysis of linear parameter varying systems using integral quadratic constraints," submitted to the 2014 ACC Conf.
[10] A. Megretski and A. Rantzer, "System analysis via integral quadratic constraints," *IEEE TAC*, vol. 42, pp. 819–830, 1997.
[11] C. Scherer, "Gain-scheduled synthesis with dynamic positive real multipliers," in *IEEE CDC Conf.*, 2012.
[12] I. Kose and C. Scherer, "Robust $\mathscr{L}_2$-gain feedforward control of uncertain systems using dynamic IQCs," *Int. J. Robust. Nonlinear Control*, vol. 19, no. 11, pp. 1224–1247, 2009.
[13] A. Megretski, "KYP lemma for non-strict inequalities and the associated minimax theorem," Arxiv, 2010.
[14] W.-Y. Yen, "Effects of Dynamic Aeroelasticity on Handling Qualities and Pilot Rating," Ph.D. Dissertation, Purdue University, 1977.
[15] P. A. Roberts, R. L. Swaim, D. K. Schmidt, and A. J. Hinsdale, "Effects of Control Laws and Relaxed Static Stability on Vertical Ride Quality of Flexible Aircraft," NASA Tech. Rep. 143843, 1977.
[16] M. R. Waszak, J. B. Davidson, and D. K. Schmidt, "A Simulation Study of the Flight Dynamics of Elastic Aircraft, Results and Analysis," NASA Tech. Rep. 4102, 1987.
[17] M. R. Waszak and D. K. Schmidt, "Flight dynamics of aeroelastic vehicles," *Journal of Aircraft*, vol. 25, no. 6, pp. 563–571, Jun. 1988.
[18] D. K. Schmidt and D. L. Raney, "Modeling and Simulation of Flexible Flight Vehicles," *AIAA JGCD*, vol. 24, no. 3, pp. 539–546, 1998.
[19] Wykes, Borland, Klepl, and MacMiller, "Design and Development of a Structural Mode Control System," NASA Tech. Rep. 143846, 1977.
[20] Wykes, Byar, MacMiller, and Greek, "Analyses and Test of the B-1 Aircraft Structural Mode Control System," NASA Tech. Rep. 144887, 1980.
[21] A. Marcos and G. Balas, "Development of Linear Parameter-Varying Models for Aircraft," *AIAA JGCD*, vol. 27, no. 2, pp. 218–228, 2004.
[22] A. Hjartarson, P. Seiler, A. Packard, and G. Balas, "LPV Aeroservoelastic Control using the LPVTools Toolbox," in *AIAA AFM Conf.*, 2013.